Solid Freeform Fabrication of Soybean Oil-Based Composites Reinforced with Clay and Fibers

Zengshe Liu[a], Sevim Z. Erhan[a,*], and Paul D. Calvert[b]

[a]Food and Industrial Oil Research, NCAUR, ARS, USDA, Peoria, Illinois 61604, and

[b]Arizona Materials Laboratories, Department of Materials Science and Engineering, University of Arizona, Tucson, Arizona 85712

ABSTRACT: Soybean oil/epoxy-based composites were prepared by an extrusion freeform fabrication method. These composites were reinforced with a combination of organically modified clay and fibers. The intercalated behavior of the epoxy resin in the presence of organo-modified clay was investigated by X-ray diffraction and transmission electron microscopy. The mixture of epoxidized soybean oil and EPON® 828 resin was modified with a gelling agent to solidify the materials until curing occurred. The flexural modulus reached 4.86 GPa with glass fiber reinforcement at 50.6 wt% loading. It was shown that the fiber orientation followed the direction of motion of the writing head that deposited the resins and had an influence on the properties of the composite. The composites cured by curing agent Jeffamine EDR-148 were found to have lower mechanical properties than those cured with triethylenetetramine, diethylenetriamine, and polyethylenimine. In addition, the effects of clay loading and fiber loading on mechanical properties of the composites were studied and reported.

Paper no. J10530 in *JAOCS 81,* XXX–XXX (June 2004).

KEY WORDS: Clay, epoxidized soybean oil, epoxy resin, fibers, solid freeform fabrication.

The major problems in engineering applications of polymers are low stiffness and strength when compared to metals. To offset these deficiencies, composite materials are prepared by adding reinforced particles or fibers to the resin. Clay is an inexpensive natural mineral, so it has been used as a filler for rubber and plastic for many years. Its reinforcing ability is poor, however, so it can be used only for conventional microcomposites. In the early 1990s, Toyota researchers (1) discovered that treatment of a montmorillonite clay with amino acids allowed dispersion of the individual 1 nm-thick silicate layers of the clay on a molecular scale in polyamid 6. Their hybrid material showed major improvements in physical and mechanical properties even at very low clay content (1.6 vol%). Polymer-clay nanocomposites also provided enhanced barrier properties (2) and reduce flammability (3). Clay and inorganic reinforcements are effective reinforcements in nanocomposite structures, but very little work has been done on using nanocomposites as a matrix in advanced fiber-reinforced composites (4,5). Hussain *et al*. (6) incorporated micro- and nanoscale Al_2O_3 particles in filament-wound carbon fiber/epoxy composites and observed an increase in modulus, flexural strength, interlaminant shear strength, and fracture toughness when the matrix was filled at 10 vol% with alumina particles (25 nm diameter). This effect stemmed largely from the large surface area of the filler and ability of the particles to interlock mechanically with the fibers. Work by Hayes *et al*. (7) has shown that nanosized alumina structures can be incorporated in the matrix and interlayer region of carbon fiber/epoxy composites. Timmerman *et al*. (8) studied the effects of layered inorganic clay incorporated into the matrices of carbon fiber/epoxy composites on the response of these materials to cryogenic cycling. They found that the laminates containing nanoclay reinforcement in the proper concentration exhibited considerably less microcracking than the unmodified or macroreinforced materials as a response to cryogenic cycling. Researchers demonstrated the feasibility of nanoparticle reinforcement, but more work remains to be performed to understand how clay and fiber reinforcements affect material properties.

During the last few years, there has been a growing interest in the use of polymers obtained from renewable resources because of their inherent advantages such as inexpensive production cost and their possible biodegradability (9). Among products from agricultural resources, vegetable oils may constitute raw materials useful in polymer synthesis. Therefore, development of cheap, biodegradable polymeric materials from soybean oil has interested many researchers.

In our previous study (10), we reported the preparation of epoxidized soybean oil (ESO)-based composites. These composites reinforced with glass, short carbon, Franklin Fiber® H-45, and Fillex® 17-AF1 fibers had thermophysical and mechanical properties comparable to petroleum-based soft rubbery polymeric materials. To obtain a variety of viable polymeric materials ranging from elastomers to rigid plastics to meet a wide variety of market demands, a combination of ESO and epoxy resin was considered. The high-strength and -stiffness composites were prepared through fiber reinforcement (Liu, Z.S., S.Z. Erhan, and P.S. Calvert, unpublished data). The method used to prepare these soy-based composites was the solid freeform fabrication (SFF) method. SFF is a method of making shapes without molds. Developed at the

*To whom correspondence should be addressed at Food and Industrial Oil Research, NCAUR, ARS, USDA, 1815 N. University St., Peoria, IL 61604. E-mail address: erhansz@ncaur.usda.gov

University of Arizona in collaboration with Advanced Ceramic Research (Tucson, AZ) (11), extrusion SFF functions as a 3-D pen plotter. The shape to be produced may be derived from a 3-D computer-aided design program or from standard drawing packages. This method has the potential to produce new materials and complex composites that cannot be made in any other way. The SFF method is important for the rapid production of prototypes and molds. This approach will also allow new combinations of materials to be formed. Further exploration of the chemical and material aspects of SFF methods was addressed by Calvert and Crockett (12). In this study, we incorporated nanoclay into ESO/epoxy composites with fiber reinforcement. The effects of clay loading and fiber loading and of fiber orientation on their properties were investigated. The SSF was used to make objects for mechanical property tests.

EXPERIMENTAL PROCEDURES

Materials. The resin used as a co-matrix, EPON® 828, was purchased from Shell Chemical Company (Houston, Texas). EPON® 828 resin is a bisphenol A/epichlorohydrin-based epoxy resin, which is the most widely used epoxy resin. ESO (7.0% oxirane oxygen) was purchased from Alf Atochem Inc. (Philadelphia, PA). Organically modified montmorillonite clay (Cloisite 30B) containing the methyl tallow bis-2-hydroxyethyl ammonium cation at a loading of 90 meq/100 g was received from Southern Clay Products (Gonzales, TX). Calcium sulfate microfiber, Franklin Fiber® H-45, wollastonite mineral fiber, Fillex® 17-AF1 fiber, and milled E-glass (electric glass) fiber are the same as described previously (10, unpublished data). Short carbon fiber, purchased from Dupont Co. (Wilmington, DE), was chopped in a coffee grinder for 20 s to reduce the length. Optical microscopy showed that the average particle length was 0.12–0.25 mm. Freire (13) studied the length distributions, diameter distributions, and aspect ratios of the fibers chopped in this method. Curing agent (triethyleneglycol diamine) Jeffamine EDR-148 was obtained from Huntsman Corporation (Houston, TX). Polyethylenimine (linear) (PEI), diethylenetriamine (DETA), and triethylenetetramine (TETA) were purchased from Aldrich Chemical Inc. (Milwaukee, WI). The chemical structures of these curing agents are shown in Scheme 1.

Forming of composites. ESO and EPON® 828 were mixed in a weight ratio of 1:0.30. Samples were placed in a 60°C oven, and vacuum was applied for 15 min to remove air bubbles. The appropriate amount of clay was added, and the mixture was stirred for 30 min and then degassed for 15 min. The mixture was sonicated for 1 h at 60°C using an Elma 9331, 300-W, 60-Hz ultrasonic cleaner (Lab-Line Instruments Inc., Melrose Park, IL). The designated fiber was added to the mixture with mechanical stirring for 30 min, and the mixture was degassed for 15 min and sonicated for 1.5 h at 60°C. The curing agent was then added and stirred for 0.5 h. The subsequent degassing and sonication steps were the same as described above. The fiber-filled slurries showed a yield point such that formed parts held their shape until cured. The mixture was removed from the oven and cooled to room temperature. The paste was put into 20-cc plastic syringes. Bars $75 \times 8 \times 4$ mm were formed by deposition of five layers and subsequently cured at 100°C for 24 h, then at 150°C for 48 h.

SFF. SFF was conducted using an Asymtek (Carlsbad, CA) model 402 fluid dispensing system, equipped with small stepper motors (Oriel stepper mike) to drive the delivery syringe. The Asymtek and syringes were controlled by a program written in Microsoft Quick Basic. Solid bar samples were written as a series of lines.

Scanning electron microscopy (SEM). SEM was performed with a JEOLJSM 6400V instrument to investigate the interface between the filler and the polymeric matrix. The specimens were mounted on aluminum stubs with graphite-filled tape, vacuum-coated with gold-palladium on a JEOL ion sputter coater, and observed. SEM micrographs were obtained using 5 kV secondary electrons.

X-ray diffraction (XRD). Powder XRD analyses were performed using a Philips 1830 diffractometer operated at 40 kV, 30 mA, with graphite-filtered CuK_α ($\lambda = 0.154$ nm) radiation and a θ compensating slit. Data were acquired in $2\theta = 0.050°$, 4-s steps. The scanning range was from 2.5 to 10°.

Transmission electron microscopy (TEM). TEM specimens were cut from nanocomposite blocks using an ultramicrotome (Sorvall MT-2 ultramicrotome) equipped with a diamond knife. Transmission electron micrographs were taken with a Hitachi HF 2000 at an acceleration voltage of 200 kV.

Mechanical testing. The mechanical properties were tested using a three-point bend test method with an Instron (Canton, MA) model 1100. The standard formula for the modulus, E and strength, σ in three-point bending of a beam was used:

$$E = PL^3/4bd^3\,\delta, \quad \sigma = 3PL/2bd^2 \qquad [1]$$

P is the maximum load applied, L is the span length, δ is the deformation at the center under load P, d is the sample height, and b is the sample width. Five specimens were tested for each set of samples, and the mean values were calculated (range ± 10% on strength and modulus).

RESULTS AND DISCUSSION

Dispersibility of clay in the ESO/epoxy resin matrix. XRD was used to examine the dispersibility of clay in the ESO/epoxy resin matrix. Figure 1 shows XRD patterns of the Cloisite 30B clay (solid line) and nanocomposites obtained from ESO/epoxy resin with 10 wt% of Cloisite 30B (dotted line) without fiber (to prevent interference of fiber in the XRD pattern). The results show a peak at $2\theta = 4.7°$ for the organoclay, which was assigned to the (001) lattice spacing of montmorillonite. The lattice spacing corresponded to an interlayer spacing of organophilic montmorillonite. Therefore, the interlayer spacing of Cloisite 30B was 18.8 Å according to $2d\sin\theta = n\lambda$. But this peak disappeared completely after reaction of the clay with epoxy resin. Although it is common

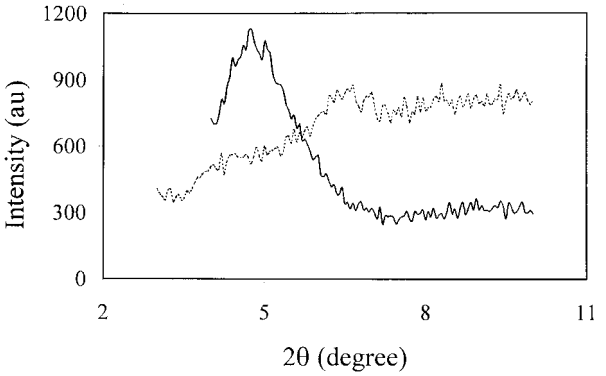

FIG. 1. X-ray diffraction patterns of (A) Cloisite 30B clay (——) and (B) Cloisite 30B clay (10 wt%) in epoxidized soy oil (ESO) (·····).

practice to classify a nanocomposite as fully exfoliated from the absence of (001) reflections, it is difficult for XRD to reveal definitive conclusions about the defined structure. Thus, TEM techniques are necessary to characterize the composites. The TEM micrograph (Fig. 2) shows that there was no aggregation of organoclay particles. This suggested that the organophilic clay was well dispersed with the ESO/ EPON matrix. Layer spacing of the clay in the nanocomposites increased by about 2 nm when compared with the organo-clay galleries. The TEM micrograph also revealed a more complex situation: There was a distribution in basal spacings. A wide distribution in basal spacings may cause the absence of the (001) reflection, so further study will be needed. Overall, an intercalated structure of the composites was developed.

Composite morphology. SEM was performed to characterize the morphology of ESO/epoxy composite materials. Characterization and SEM micrographs of four types of fibers used in our experiments have been reported previously (10). Figure 3 shows SEM of a freshly fractured surface for an ESO/EPON 828/clay composite filled with these fibers. Figures 3A–D correspond to milled glass fiber, Franklin

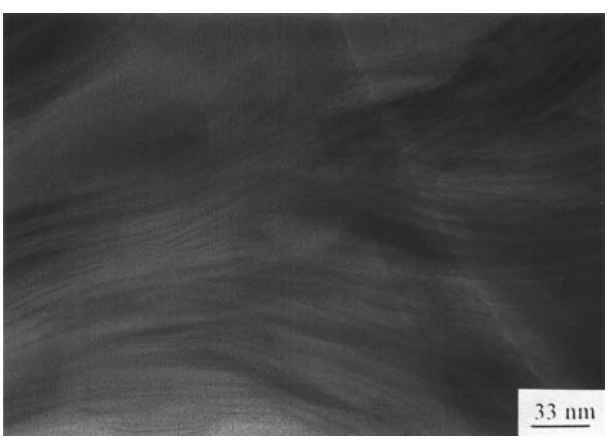

FIG. 2. Transmission electron micrograph of ESO/EPON® 828/organoclay composites. EPON® 828 furnished by Shell Chemical (Houston, TX). For abbreviation see Figure 1.

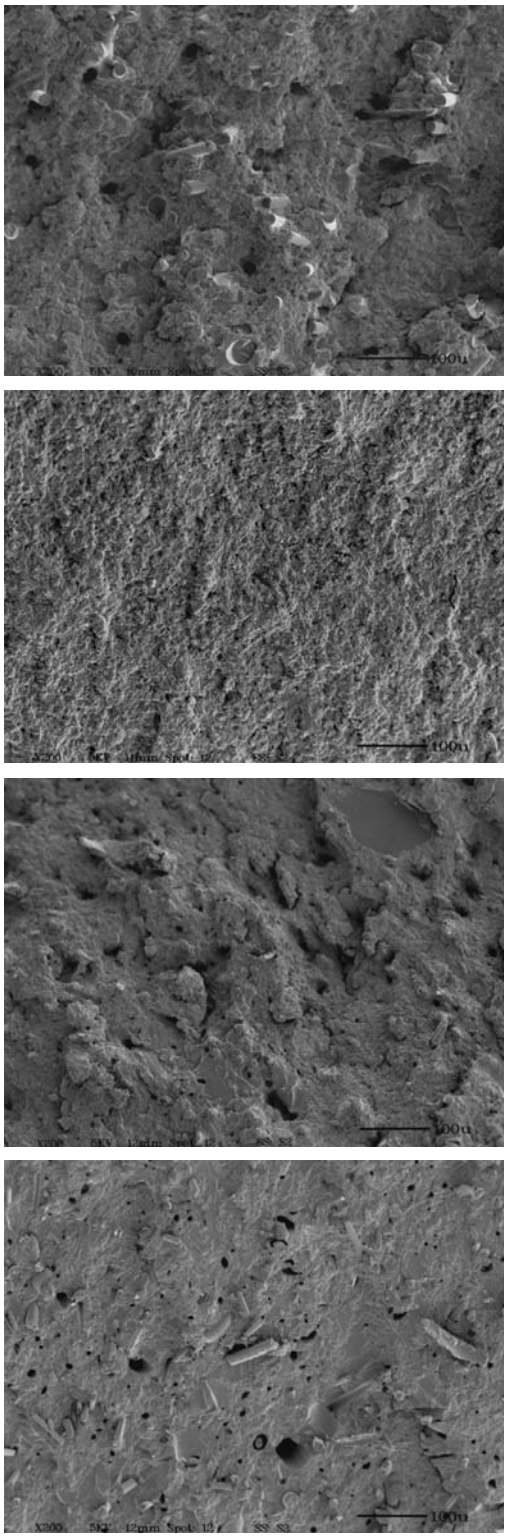

FIG. 3. Scanning electron micrographs of the freshly fractured surface of ESO/epoxy-based composites filled with four kinds of fiber. Composite filled with (A) E-glass fiber, (B) Franklin Fiber® H-45, (C) wollastonite, Fillex® 17-AF1 fiber, and (D) carbon fiber.

Fiber® H-45, Fillex® 17-AF1 fiber, and carbon fiber, respectively. They clearly indicate that interfacial adhesion between the fiber and matrix exists. This can be readily seen from the physical contact between both components. The fibers are broken up from the matrix. However, holes and spacing occur along the fiber, resulting in poor contact and inferior stress transfer between the phases.

Effect of curing agents. Four kinds of amine compounds, as shown in Scheme 1, were selected as curing agents for the ESO/EPON system. Table 1 presents flexural strength and modulus data for the composites cross-linked with these curing agents. The molar ratio of epoxide (the contribution from ESO and EPON® 828) to hydrogen (from the curing agent) was 1:1.67. The curing agents TETA and DETA produced composites with better mechanical properties than Jeffamine EDR-148. J. Xu and colleagues (J. Xu, Z.S. Liu, S.Z. Erhan, and C.J. Carriere, unpublished data) investigated viscoelastic properties of materials made from ESO cross-linked by TETA and Jeffamine EDR-148. They also found that the ESO-based material cross-linked by the TETA had a higher glass transition temperature and stronger viscoelastic solid properties than the ESO-based material cross-linked by the Jeffamine EDR-148. By comparing structures of these curing agents, it is clear that there are two primary amine groups located on the two ends of the TETA and DETA chains. There is also one additional active site, i.e., the secondary amine group, in the middle of the DETA chain and two secondary amine groups in the middle of the TETA chain. On the other hand, there is no secondary amine group in Jeffamine EDR-148. These secondary amine groups behaved as a "short arm" and contributed to the formation of a 3-D thermoset network. The network structure of the polymer matrix provided strong mechanical properties of the composites. Also, owing to the presence of many secondary amine groups in the backbone of the PEI molecule, better mechanical properties of the composites could be obtained.

TABLE 1
Effect of Curing Agents[a]

Curing agent	Flexural strength (MPa)	Flexural modulus (GPa)	Strain at break (%)
Jeffamine EDR-148	55	0.11	1.3
PEI	85	1.89	1.1
DETA	120	1.70	1.9
TETA	195	2.57	2.2

[a]Conditions: Epoxodized soy oil (ESO), 57.5 wt%, EPON® 828 (Shell Chemical Co., Houston, TX), 17.5 wt%; Franklin Fiber®, 25.0 wt%, and clay, 10 wt% (ESO + EPON 828 + clay).

Effect of fiber type. The improvement of mechanical and thermal properties of fiber plastics depends on factors such as variation in the mobility of the macromolecules in the boundary layers, influence of the orientation of the fiber surface, the effect of fibers on the structure of the polymers, as well as the different types of fiber–polymer interactions. Fiber types influence the properties of the composites. In general, the mechanical and physical properties of natural fiber-reinforced plastics only conditionally reach the characteristic values of glass fiber-reinforced systems. In this clay-reinforced polymeric matrix system, the influences of fiber type (Franklin Fiber® H-45, Fillex® 17-AF1 fiber, short carbon filter, and milled E-glass fiber) on the mechanical properties of the composites were explored. The results of the mechanical property measurements are presented in Table 2. Among the different types of fibers, glass and carbon fibers had slightly better reinforcing effects than mineral fibers. These results are probably due to the inherently high strength of glass and carbon fibers. For example, E glass fiber has a tensile strength of about 3 GPa and a modulus that approaches 100 GPa. This provides a large contribution to the strength and rigidity of

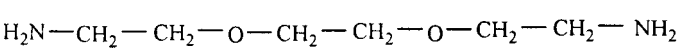

Jeffamine EDR-148

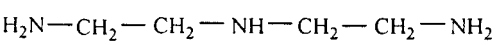

Diethylenetriamine (DETA)

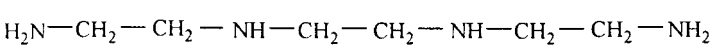

Triethylenetetramine (TETA)

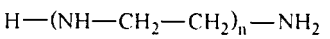

Polyethylenimine, linear (PEI)

SCHEME 1

TABLE 2
Effect of Different Types of Fibers

Fiber	Flexural strength (MPa)	Flexural modulus (GPa)	Strain at break (%)
E-glass	150	2.59	1.7
Carbon	153	2.61	1.7
Franklin H-45	195	2.57	2.2
Fillex 17-AF1	130	2.24	1.8

the reinforced composites. The principal advantages of glass fibers commonly used as reinforcing fibers for a polymer matrix are their high strength and their low cost.

Influence of fiber orientation on flexural modulus. The strength and moduli of fiber-reinforced composites depend not only on the fiber volume fraction and aspect ratio but also on their orientation. When the fibers are aligned longitudinally, the maximal stress transfer occurs between the fiber and matrix. The maximal strength and reinforcement are achieved along the direction of fiber alignment. There are good theoretical treatments for the effect of aspect ratio and volume fraction on modulus (14), but orientation is more difficult to control. It is strongly influenced by processing methods and by local flow conditions in, for instance, injection-molded parts. As a result, changes in the volume fraction and aspect ratio will change the degree of orientation. Also, theoretical treatments are not very satisfactory. Calvert and colleagues (15,16) studied orientation effects in freeformed short-fiber composites. Optical microscopy was used to measure the major and minor axes of the elliptical fiber sections. They discovered that fiber orientation corresponded closely to the machine direction during sample preparation. In glass fiber/epoxy composites, they found that 90% of fibers were within 10° of the machine's writing direction. By writing a series of test bars with writing axes at different angles to the long axis, the modules could be varied by approximately a factor of three. In this ESO/epoxy/clay system, we prepared test bars by writing at varying angles relative to the axis of the test bars to investigate effects of fiber orientation on the properties of composites. The effect of this orientation on the flexural moduli is shown in Table 3. The flexural moduli were found to be slightly higher at writing angles parallel to the long axis than across the long axis. This difference between longitudinal and transverse moduli is similar in many types of composites. However, this difference is less significant in a

TABLE 3
Effect of Orientation on EPON 828/ESO/TETA[a] Reinforced with Franklin Fiber® H-45 25 wt% and Clay 10 wt%

Fiber orientation	Flexural strength (MPa)	Flexural modulus (GPa)	Strain at break (%)
0	195	2.57	2.2
30	190	2.55	1.4
45	180	2.50	1.3
60	170	2.35	1.3
90	167	2.32	1.5

[a]Conditions: ESO, 57.5 wt% and EPON 828, 17.5 wt%. For manufacturer see Table 1. TETA, triethylaminetetramine; for other abbreviation see Table 1.

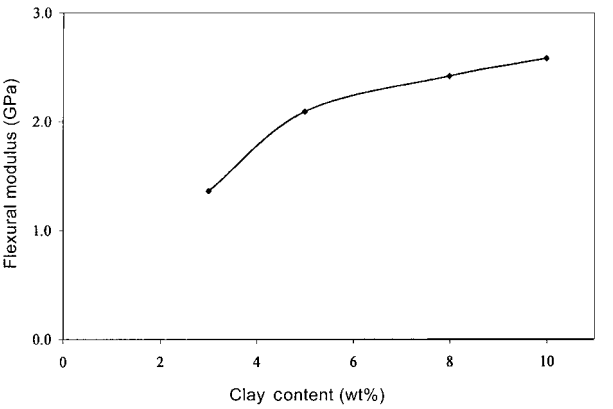

FIG. 4. Flexural modulus of composites as a function of clay content.

clay/fiber reinforced system. A possible explanation is that the higher viscosity of matrix slurry, reinforced by nanoclay, increases slurry–fiber interaction and the fiber orientation is restricted.

Effects of clay loading. The effects of clay loading on the mechanical properties of composites are shown in Figure 4. The flexural modulus of a composite increased rapidly with increasing clay content from 2 to 5 wt%, resulting in a change from 0.78 to 2.09 GPa. Thereafter, the increase was slow. Liu and Wu (17) also reported a similar phenomenon in polypropylene/clay nanocomposites prepared by the grafting-melt compounding method. The nanometric dispersion of silicate layers in the matrix led to improved modulus and strength. The stiffness of the silicate layers contributed to the presence of immobilized or partially immobilized polymer phases. Silicate layer orientation as well as molecular orientation also contributed to the observed reinforcement effects. The slow increase of the flexural modulus at higher clay contents (above 5 wt%) can be attributed to the inevitable aggregation of the clay layers.

Effect of fiber loading. The flexural moduli of composites as a function of Franklin Fiber® H-45 and glass fiber content are presented in Figures 5 and 6, respectively. In Figure 5, the flexural modulus increased rapidly from 2.04 to 3.34 GPa

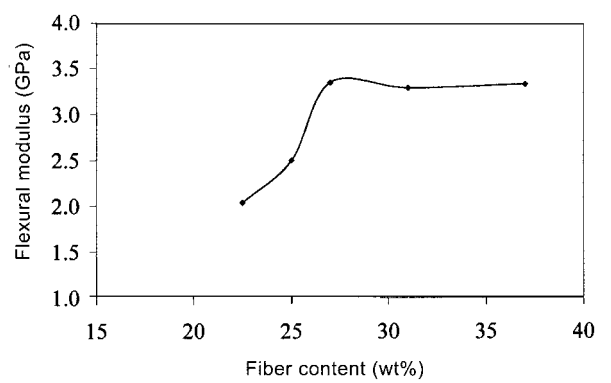

FIG. 5. Flexural modulus of composites as a function of Franklin Fiber® H-45 fiber content.

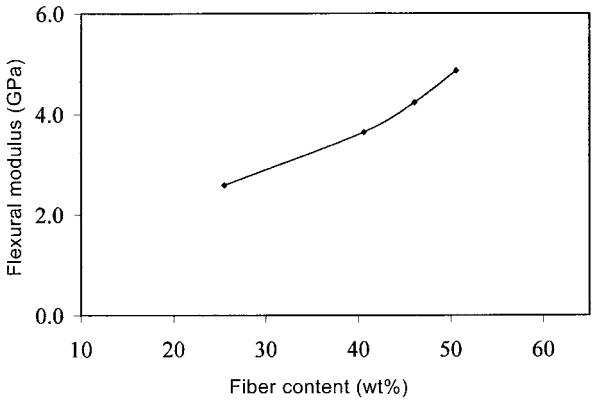

FIG. 6. Flexural modulus of composites as a function of glass fiber content.

with an increase in fiber content from 22.5 to 27 wt%. When the fiber fraction increased beyond 27 wt%, the flexural modulus tended to stabilize. This stabilization was due to increased fiber-to-fiber interactions at a higher fiber fraction, leading to fiber dispersion problems. Also, it was more difficult to impregnate the fiber with prepolymer, which in turn can make the fiber distribution in the matrix less homogeneous. However, the flexural modulus increased consistently with glass fiber content (Fig. 6). The flexural modulus reached 4.86 GPa at a glass fiber loading of 50.6 wt%. This glass fiber-reinforced composite did not have maximal mechanical properties because the step motor in our SFF system was insufficient to allow the highly viscous slurry to flow through the needle. Although the data for higher glass fiber fractions are not available, it is predicted that the maximized flexural modulus of glass fiber-reinforced composites will be obtained at an even higher fiber content.

ACKNOWLEDGMENTS

The authors gratefully acknowledge Drs. Arthur Thompson and Jinguo Wang for their help in SEM and TEM micrographs and Gary Grose for XRD measurements.

REFERENCES

1. Okada, A., M. Kawasumi, A. Usuki, Y. Kojima, T. Kurauchi, and O. Kamigaito, Nylon 6-Clay Hybrid, *Mater. Res. Soc. Proc. 171*:45–50 (1990).
2. Kojima, Y., A. Fujushima, A. Usuki, A. Okada, and T. Kurauchi, Gas Permeabilities in Rubber-Clay Hybrid, *J. Mater. Sci. Lett. 12*:889–890 (1993).
3. Giannelis, E.P., Polymer Layered Silicate Nanocomposites, *Adv. Mater. 8*:29–34 (1996).
4. LeBaron, P.C., Z. Wang, and T.J. Pinnavaia, Polymer-Layered Silicate Nanocomposites: An Overview, *App. Clay Sci. 15*: 11–29 (1999).
5. Alexandre, M., and P. Dubois, Polymer-Layered Silicate Nanocomposites: Preparation, Properties and Uses of a New Class of Materials, *Mater. Sci. Eng. 28*:1–63 (2000).
6. Hussain, M., A. Nakahira, and K. Niihara, Mechanical Property Improvement of Carbon Fiber Reinforced Epoxy Composites by Al_2O_3 Filler Dispersion, *Mater. Lett. 26*: 185–191 (1996).
7. Hayes, B.S., M. Nobelen, A.K. Dharia, and J.C. Seferis, Evaluation of Microcracking in Aerospace Composites Exposed to Thermal Cycling: Effect of Composite Lay-up, Laminate Thickness and Thermal Ramp Rate, *33rd International SAMPE Technical Conference*, Society for the Advancement of Material and Process Engineering, Covina, CA 2001, pp. 120–128.
8. Timmerman, J.F., B.S. Hayes, and J.C. Seferis, Cryogenic Microcracking of Nanoclay Reinforced Polymeric Composite Materials, *47th International SAMPE Symposium,* Society for the Advancement of Material and Process Engineering, Covina, CA 2002, pp. 1119–1130.
9. Kaplan, D.L., *Biopolymers from Renewable Resources,* Springer, New York, 1998.
10. Liu, Z.S., S.Z. Erhan, J. Xu, and P.D. Calvert, Development of Soybean Oil-Based Composites by Solid Freeform Fabrication Method: Epoxidized Soybean Oil with Bis or Polyalkyleneamine Curing Agents System, *J. Appl. Poly. Sci. 85*: 2100–2107 (2002).
11. Stuffle, K., A. Mulligan, P. Calvert, and J. Lombardi, Solid Freebody Forming from Polymerizable Slurry, *Proceedings of the Solid Freeform Fabrication Symposium,* University of Texas, Austin, 1994, pp. 60–63.
12. Calvert, P., and R. Crockett, Chemical Solid Free-Forming Fabrication: Making Shapes without Molds, *Chem. Mater. 9*:650–663 (1997).
13. Freire, R.S., Short Fiber Composites with High Electrical and Thermal Conductivity, M.S. Thesis, The University of Arizona, Tucson, 1992.
14. Hull, D., and T.W. Clyne, *An Introduction to Composite Materials,* Cambridge University Press, Cambridge, 1996.
15. Peng, J., T.L. Lin, and P. Calvert, Orientation Effects in Freeformed Short-Fiber Composites, *Composites A 30*:133–138 (1999).
16. Calvert, P., J. Peng, and C. Souvignier, Solid Freeform Fabrication of Composites by Direct Deposition and by *in situ* Mineralization, *Mater. Res. Soc. Symp. Proc. 542* (Solid Freeform and Additives):3–11 (1999).
18. Liu, X.H., and Q.J. Wu, PP/Clay Nanocomposites Prepared by Grafting–Melt Intercalation, *Polymer 42*:10013–10019 (2001).

[Received December 23, 2002; accepted April 20, 2004]